

## Magnetic field chaos in the Sherrington-Kirkpatrick model

Alain Billoire and Barbara Coluzzi

*Service de Physique Théorique CEA-Saclay, Orme des Merisiers, 91191 Gif-sur-Yvette, France*

(Received 24 October 2002; published 17 March 2003)

We study the Sherrington-Kirkpatrick model, both above and below the de Almeida-Thouless line, by using a modified version of the Parallel Tempering algorithm in which the system is allowed to move between different values of the magnetic field  $h$ . The behavior of the probability distribution of the overlap between two replicas at different values of the magnetic field  $h_0$  and  $h_1$  gives clear evidence for the presence of magnetic field chaos already for moderate system sizes, in contrast to the case of temperature chaos, which is not visible on system sizes that can currently be thermalized.

DOI: 10.1103/PhysRevE.67.036108

PACS number(s): 02.60.-x, 75.10.Nr, 75.40.Mg

### I. INTRODUCTION

The Sherrington-Kirkpatrick (SK) model was introduced quite a long time ago [1] as a mean-field model for spin glasses. Its proposed analytical solution [2] displays intriguing features such as an infinite number of pure states in the glassy phase, described by an order parameter, which is the nontrivial probability distribution of the overlap between two states,  $P(q)$ . After more than 20 yr this solution is still the subject of works aiming at establishing it in full mathematical rigor [3,4], whereas long standing open issues concern the study of the corrections to the mean-field approximation below the upper critical dimension [5] and the very applicability of the mean-field picture to short range realistic spin glasses [6].

An interesting question concerns the way in which the states reorganize themselves when the system is subjected to a small perturbation  $\delta p$  of an external parameter, in particular, the temperature  $T$  or the magnetic field  $h$ . There is the intriguing possibility of  $p$  chaos, namely, the states at  $p$  and  $p + \delta p$  are as different as possible in the thermodynamic limit.

The possible presence of temperature chaos in the SK and related models is an old subject of investigations [7–10] that recently received a lot of attention both analytically and numerically [11–16]. From a very recent analytical computation [17] it turns out to be present, but to be of the ninth order in perturbation theory, a very weak effect, extremely difficult to be numerically observed on the system sizes one is currently able to thermalize.

The aim of this paper is to investigate the appearance of chaos with increasing system sizes (a question that cannot be addressed by the existing analytical techniques that are restricted to the asymptotic  $N \rightarrow \infty$  regime), in a case where chaos is strong, namely, the case of magnetic field chaos. The presence of magnetic field chaos was predicted already 20 years ago [18] (see also [7,10]). From the numerical point of view, it was observed in a previous work [9] from a study of the behavior of the second moment of the probability distribution of the overlap  $P_{h_0, h_1}(q)$  between replicas at  $h_0 = 0$  and  $h_1 \neq 0$ . This pioneering paper can, however, be criticized, since many data points are on the wrong side of the de Almeida-Thouless (AT) line [19]. We will revisit the problem

by looking (in the SG phase) at the distribution  $P_{h_0, h_1}(q)$  itself, a quantity whose interpretation is simpler than the moments.

More in detail, in terms of the probability distribution of the overlap between two replicas at different values of the external parameter  $h_0$  and  $h_1 = h_0 + \delta h$ , chaos has a very clean signature. Taking for simplicity the case  $h_0 = 0$ , for small volumes,  $P_{0, \delta h}(q)$  has two peaks, and is very similar to  $P_{0,0}(q)$  on the same volume. As the volume grows, a peak develops around the minimal value of the overlap  $q_m = 0$ , in such a way that for very large volumes  $P_{0,0}(q) \approx \delta(q)$ . In the temperature chaos case, this chaotic peak is hardly visible with current computers and algorithms. Our aim is to determine if and how this “chaos peak” scenario takes place in the case of  $h$  chaos, which is believed to be much stronger than  $T$  chaos.

To this aim, we perform numerical simulations of the SK model at  $T = 0.6T_c$ , both above and below the AT line, by using a modified version of the Parallel Tempering (PT) algorithm [20,21] in which the system is allowed to move between different  $h$  values at fixed temperature.

### II. MODEL AND OBSERVABLES

The Sherrington-Kirkpatrick spin glass model [22,23] is described by the Hamiltonian

$$\mathcal{H}_J = \sum_{1 \leq i < j \leq N} J_{ij} \sigma_i \sigma_j - h \sum_{1 \leq i \leq N} \sigma_i, \quad (1)$$

where  $\sigma_i = \pm 1$  are Ising spins, the sum runs over all pairs of spins, and  $J_{ij}$  are quenched identically distributed independent random variables with mean value  $\overline{J_{ij}} = 0$  and variance  $1/N$ . We take  $J_{ij} = \pm N^{-1/2}$ .

In order to measure the probability distribution of the overlap  $P(q)$  one usually considers two independent replicas  $\{\sigma_i\}$  and  $\{\tau_i\}$  evolving contemporaneously and independently (at the same temperature and at the same value of the magnetic field):

$$Q = \frac{1}{N} \sum_{i=1}^N \sigma_i \tau_i, \quad (2)$$

$$P(q) \equiv \overline{P_j(q)} \equiv \langle \overline{\delta(q - Q)} \rangle, \quad (3)$$

where the thermal average  $\langle \cdot \rangle$  corresponds to the average over the Monte Carlo time in the simulation, whereas  $\overline{(\cdot)}$  stands for the average over the  $J_{ij}$  realizations. This is the order parameter in the glassy phase, which in the thermodynamic limit behaves as

$$P(q) = \begin{cases} \delta(q - q_{EA}), & |h| > h_{AT}(T) \\ x_m \delta(q - q_m) + \tilde{P}(q) + x_M \delta(q - q_{EA}), & 0 < |h| < h_{AT}(T) \\ \frac{1}{2} [\tilde{P}(q) + \tilde{P}(-q)] + \frac{1}{2} x_M [\delta(q - q_{EA}) + \delta(q + q_{EA})], & h = 0, T < T_c, \end{cases} \quad (4)$$

where  $h_{AT}(T)$  is the critical value of the magnetic field signaling the AT line, with  $h_{AT}(T) \sim (4/3)^{1/2} (T_c - T)^{3/2}$  for  $T \rightarrow T_c^-$  ( $T_c = 1$  in this model) [19]. In the glassy phase, the stable solution corresponds to a full replica symmetry breaking (FRSB), i.e., to a nontrivial  $P(q)$  with a continuous distribution  $\tilde{P}(q)$  between two  $\delta$  functions at values  $q_{EA}$  and  $q_m$ , respectively. For  $T \rightarrow T_c^-$ , one finds that  $x_m \propto q_m \propto h^{2/3}$ ,  $(q_{EA} - q_m) \propto (x_M - x_m) \propto [h_{AT}(T) - h]$ . Note that at  $h = 0$  the function  $P(q)$  is symmetric, reflecting the symmetry of the system for  $\{\sigma_i\} \rightarrow \{-\sigma_i\}$ , and the  $\delta$  function in  $q_m$  disappears.

The interesting quantity to study when looking for chaos is the probability distribution of the overlap between two replicas that evolve at different values of the magnetic field,  $h_0$  and  $h_1 = h_0 + \delta h$ , definable as

$$P_{h_0, h_1}(q) = \langle \overline{\delta(q - Q_{h_0, h_1})} \rangle. \quad (5)$$

It is expected to become a  $\delta$  function in the thermodynamic limit, where, in the presence of chaos, states are as different as possible and accordingly their mutual overlap approaches the minimum possible value, i.e.,  $q_m(h_0)$  (which is zero for  $h_0 = 0$ ). This happens certainly in the  $N \rightarrow \infty$  limit as soon as the condition  $(h_1 - h_0)^2 N \gg 1$  is verified [18].

In finite dimensions, one can define the overlap correlation function  $C_{h_0, h_1}(|\mathbf{r}_i - \mathbf{r}_j|) = \langle \sigma_i \sigma_j \rangle \langle \tau_i \tau_j \rangle$ , which decays exponentially with a correlation length that was evaluated (in  $d > 8$ , i.e., above the upper critical dimension of the model) [7] to be  $\xi_{h_0=0, h_1} \propto h_1^{-2/3}$  and  $\xi_{h_0 \neq 0, h_1 = h_0 + \delta h} \propto h_0^{-1/6} (\delta h)^{-1/2}$ , respectively.

Dimensional ratios of momenta, such as

$$A^{2n}(h_0, h_1, T) = \frac{\langle (q - \langle q \rangle_{h_0, h_1})^{2n} \rangle_{h_0, h_1}}{\sqrt{\langle (q - \langle q \rangle_{h_0, h_0})^{2n} \rangle_{h_0, h_0} \langle (q - \langle q \rangle_{h_1, h_1})^{2n} \rangle_{h_1, h_1}}}, \quad (6)$$

$$B^{2n}(h_0, h_1, T) = \frac{\langle (q - \langle q \rangle_{h_0, h_1})^{2n} \rangle_{h_0, h_1}}{\langle (q - \langle q \rangle_{h_0, h_0})^{2n} \rangle_{h_0, h_0}}, \quad (7)$$

have been introduced in order to look for chaos in Ref. [9], where it was argued that they should scale as  $\tilde{f}(Nh_1^{8/3})$  for  $h_0 = 0$  and should approach zero for  $N \rightarrow \infty$ , namely, there is magnetic field chaos.

The finite size corrections to the asymptotic behavior of  $P_{h_0, h_1}(q)$  were computed in Ref. [10] by considering two replicas, at different values of the magnetic field, constrained

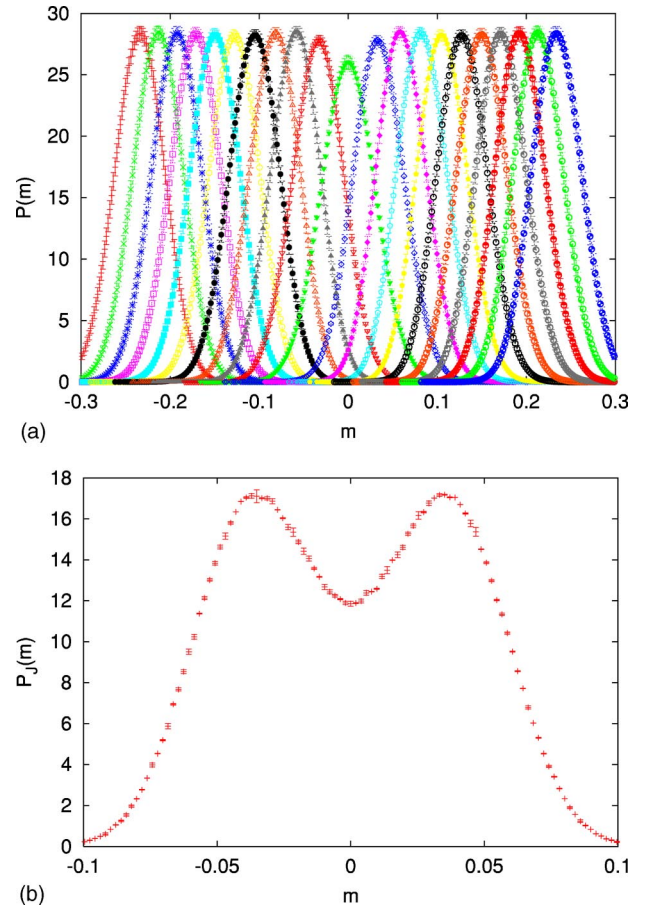


FIG. 1. In (a) we plot the disorder averaged probability distribution of the magnetization  $P(m)$  at 21 different central  $h$  values of the set (i.e., from  $h = -0.25$  to  $h = 0.25$ ) for the largest considered system sizes  $N = 1024$ . In (b) we present  $P_j(m)$  at  $h = 0$  for a two-peak sample for  $N = 1024$  again. In this last case the errors are roughly evaluated as the difference between the values measured in the second quarter and in the second half of the run.

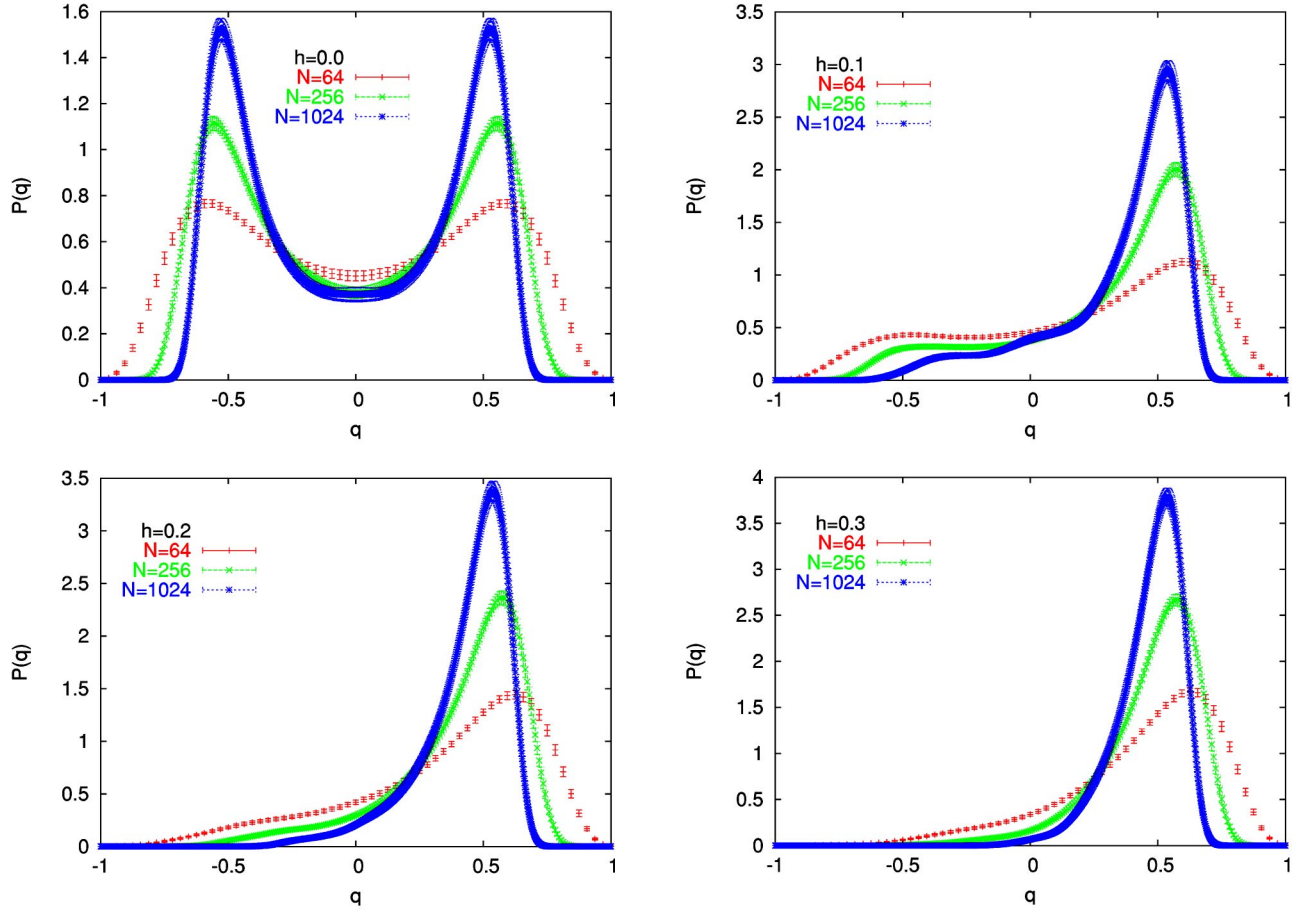


FIG. 2. The probability distribution of the overlap  $P(q)$  between two replicas evolving at  $h=0.0, 0.1, 0.2$ , and  $0.3$ , respectively, for the considered system sizes.

to have a fixed overlap  $q$ . The constraint causes a free-energy excess for  $q \neq q_m$  given by  $\Delta f = f(q = q_m + \delta q) - f(q = q_m)$ , with

$$\Delta f = \begin{cases} \left( \frac{2187}{32} \right)^{1/3} \frac{\delta q^2 h_1^{8/3}}{q_{EA}}, & h_0 = 0 \\ \frac{\delta q^2 h_0 \delta h}{\sqrt{2}}, & h_0 \neq 0, \delta h = |h_1 - h_0| \ll h_0. \end{cases} \quad (8)$$

Correspondingly, one has  $P_{h_0, h_1}(q) \propto \exp(-N\Delta f)$ , i.e., a Gaussian with variance  $\langle q^2 \rangle_{0, h_1} \propto (N h_1^{8/3})^{-1}$  for  $h_0 = 0$ , in agreement with the above scaling law.

### III. PARALLEL TEMPERING IN MAGNETIC FIELD

The PT or Multiple Markov Chain Method is a widely used numerical algorithm particularly efficient for simulating (some) systems with a corrugated free-energy landscape. The basic idea is that the system at equilibrium, instead of being trapped in a single low temperature valley is allowed to move at higher temperatures where the landscape is trivial and to return at low  $T$  in a different valley. This can be

achieved by considering  $n$  replicas of the system, each at a different temperature in a given set (of temperatures), and by allowing exchanges of temperatures between nearest neighbor replicas with the usual Monte Carlo probability.

Here we consider a set of replicas at different values of the magnetic field, both above and below the AT line, allowing exchange of  $h$  values between the nearest neighbor replicas with the appropriate probability

$$P(\{h_1, \{\sigma^1\}; h_2, \{\sigma^2\}\} \rightarrow \{h_2, \{\sigma^1\}; h_1, \{\sigma^2\}\}) = \begin{cases} 1, & \Delta H_{tot} > 0 \\ e^{\beta \Delta H_{tot}}, & \Delta H_{tot} < 0, \end{cases} \quad (9)$$

where

$$H_{tot} = \sum_{a=1}^n \sum_{1 \leq i < j \leq N} J_{ij} \sigma_i^a \sigma_j^a - h_{\pi(a)} \sum_{1 \leq i \leq N} \sigma_i^a \quad (10)$$

and therefore

$$\Delta H_{tot} = -(h_1 - h_2) \left( \sum_{i=1}^N \sigma_i^1 - \sum_{i=1}^N \sigma_i^2 \right). \quad (11)$$

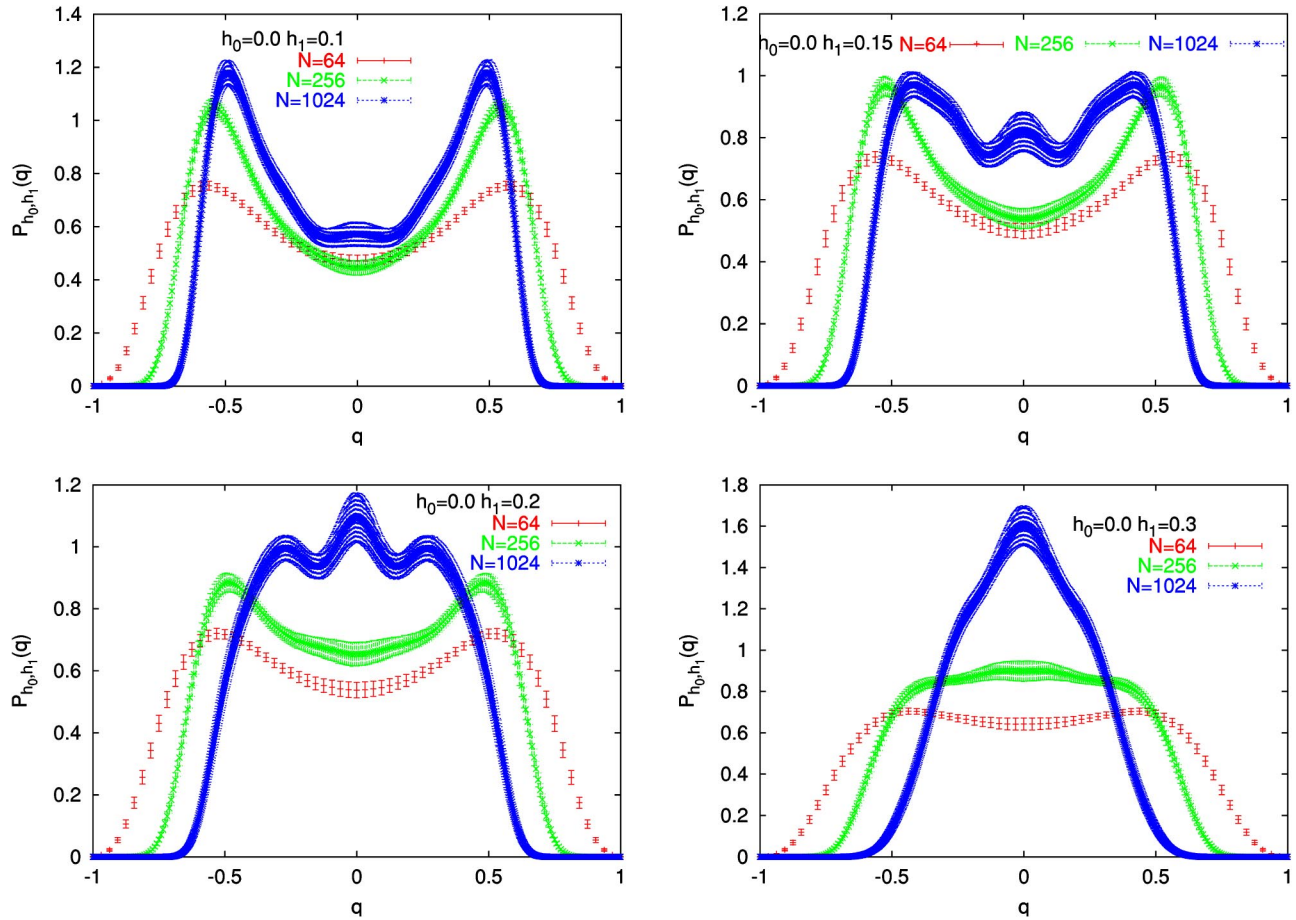


FIG. 3. The probability distribution of the overlap  $P_{h_0, h_1}(q)$  between replicas evolving at different magnetic field values, with  $h_0 = 0.0$  and  $h_1 = 0.1, 0.15, 0.2$ , and  $0.3$ , respectively, for the considered system sizes.

In principle this  $h$ -PT method should be efficient for thermalization, like the usual  $T$ -PT method, since the landscape is trivial above the AT line. It is, moreover, a well-suited method for the kind of numerical study we are interested in, since one can easily measure  $P_{h_0, h_1}(q)$  by considering two or more independent sets of replicas. However, as we are going to discuss in detail, we find that its efficiency rapidly decreases while simulating large system sizes.

We studied the cases  $N = 64, 256$ , and  $1024$ , taking a set of  $n = 49$  equally spaced magnetic field values between  $h = \pm |h_{max}| = \pm 0.6$  at the temperature  $T = 0.6$ , where the AT line occurs at the critical value  $h_{AT}(T = 0.6) \approx 0.382$  [24].

We alternate one sweep of each replica with the usual Metropolis algorithm and one sweep with the PT algorithm.

The probability of two replicas to exchange their magnetic fields is related to the overlap between the corresponding histograms of the magnetization  $P(m)$  that we check to be large enough (see Fig. 1) even for  $N = 1024$ . However, some single samples  $P_J(m)$  display two peaks at  $\pm m_0 \neq 0$  when  $h = 0$  (see Fig. 1). As a result, the replicas can separate into two distinct subsets, one evolving in the phase space with positive and the other with negative magnetic field values [the probability of a replica that arrive at  $h = 0$  with  $m \approx -m_0 < 0$  to move at a positive  $\delta h$  value is of order

$\exp(-\beta m_0 \delta h N)$ , much smaller than the usual  $\exp(-\beta \chi \delta h^2 N)$ ]. This happens for some  $N = 1024$  samples. In order to avoid such a problem, we add a possible global movement, allowing a replica at  $h = 0$  to reverse the sign of all its spins with probability  $1/2$ .

Each run is divided into two equal parts and we check thermalization by comparing the data obtained in the second part with that of the second quarter, looking in particular at the behavior of  $P_{h_0, h_1}(q)$ . We perform  $50.000 + 50.000$ ,  $100.000 + 100.000$ , and  $300.000 + 300.000$   $h$ -PT steps for  $N = 64, 256$ , and  $1024$ , respectively. In the  $N = 1024$  case we also performed independent runs with temperature PT for 64 disorder samples at  $h = 0$  and  $h = 0.3$ , obtaining indistinguishable results for  $P(q)$ .

We simulated four sets of replicas evolving simultaneously and independently (i.e.,  $49 \times 4 = 196$  replicas). Data are averaged over 256 disorder configurations for each system size, and statistical errors are evaluated from sample-to-sample fluctuations by using the jackknife method. The program was multispin coded with 64 different sites of the system in the same computer word and the whole simulations took about 5500 CPU hours (in the largest part used for  $N = 1024$ ), i.e., about one week when running over 32 pro-

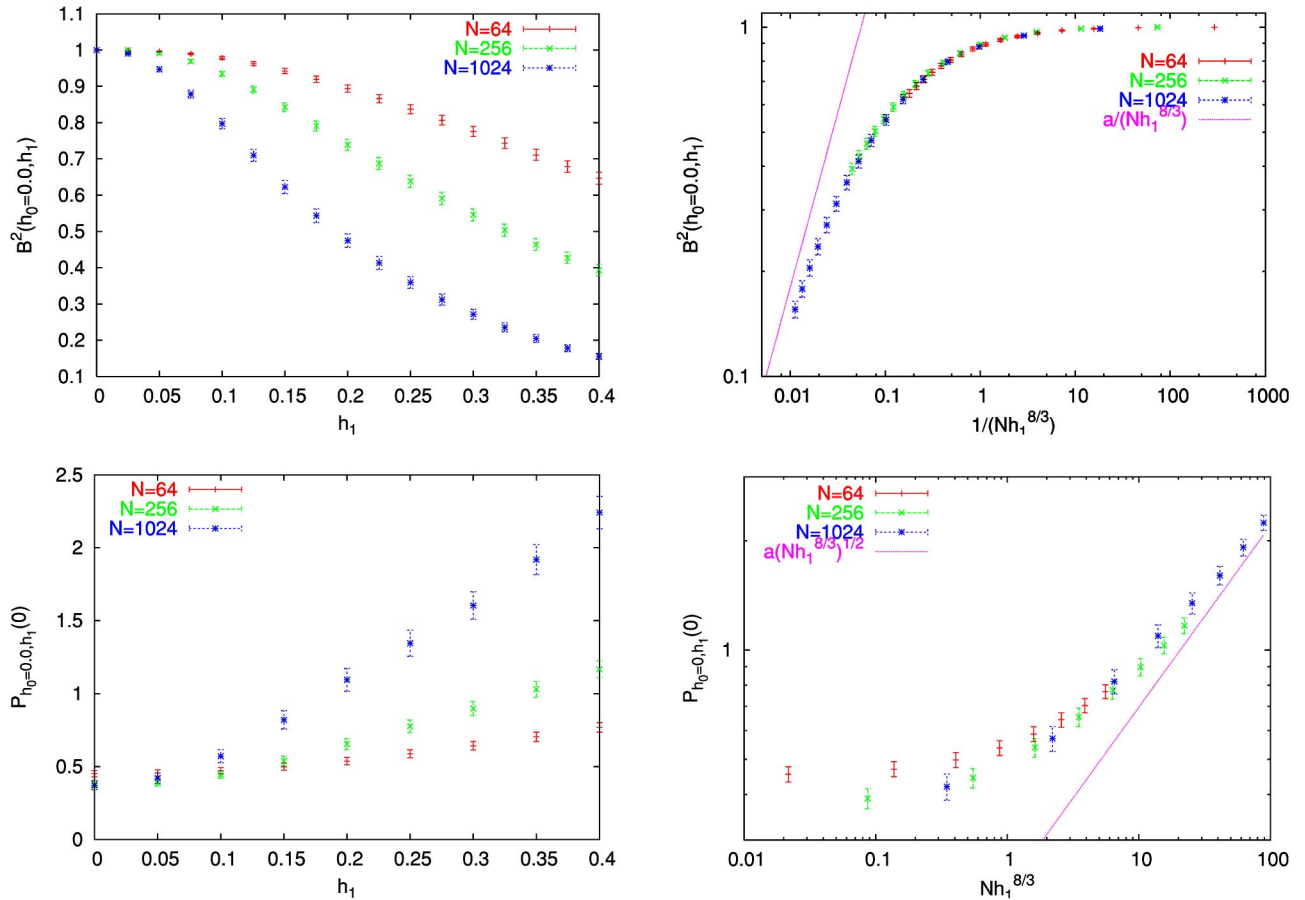


FIG. 4. On the top, the behavior of  $B^2(h_0, h_1)$  for  $h_0=0.0$  as a function of  $h_1$  (left) and as a function of the scaling variable  $1/(Nh_1^{8/3})$  compared with the asymptotic behavior  $\propto 1/(Nh_1^{8/3})$  for  $1/(Nh_1^{8/3}) \ll 1$  (log-log plot on the right). On the bottom, the behavior of  $P_{h_0, h_1}(0)$  for  $h_0=0.0$  as a function of  $h_1$  (left) and as a function of  $Nh_1^{8/3}$  compared with the asymptotic behavior  $\propto \sqrt{Nh_1^{8/3}}$  for  $Nh_1^{8/3} \gg 1$  (log-log plot on the right).

cessors on the COMPAQ SC270 (the program can be easily parallelized by running different samples over different processors).

In the  $N=64$  and 256 cases the algorithm works quite nicely, as can be seen from the number of tunnelings, namely, the number of times that each replica moves from one extremum of the set (of  $h$  values) to the other and back, which is about  $\mathcal{N}=15-20$  (in the second half of the run). On the other hand, already for  $N=1024$ , despite the 300.000 PT steps of the second part of the run, this number drops to  $\mathcal{N}=5-6$  and in nearly one-fourth of the samples there is at least one replica, which is unable to go from  $h_{max}$  to  $h_{min}$  and back, in the whole interval considered (in a few cases most replicas never did it).

In the case of temperature PT, the corresponding (average) number of tunnelings are 3780, 1590, and 455, respectively (in the runs of 400.000 steps starting from equilibrium configurations, with a set of 38 temperatures between  $T_{max}=1.325$  and  $T_{min}=0.4$  at  $h=0.3$  for  $N=64, 256$ , and 1024). Clearly the number of tunnelings decreases much faster with the system size in the  $h$ -PT case. This is presumably linked to the early appearance of magnetic field chaos. As we will discuss in detail in the following section,  $P_{h_0, h_1}(q)$  starts to approach a  $\delta$  function, i.e., its thermodynamic limit behavior,

already for magnetic field differences of order 0.15, for  $N=1024$ . This means that the corresponding phase spaces are *very* different and that an algorithm based on global movements between different values of  $h$  cannot work well. Similarly, the efficiency of temperature PT should drop down for extremely large systems due to temperature chaos finally coming out.

The bottom line is that  $N=1024$  is the largest size we are able to efficiently thermalize at  $T=0.6$  by using the  $h$ -PT algorithm, to be compared with the four times larger  $N=4096$  that can be thermalized down to  $T=0.4$  with the temperature PT algorithm at zero magnetic field.

## IV. RESULTS AND DISCUSSION

### A. On the finite size corrections to the $P(q)$

The function  $P(q)$  is shown in Fig. 2 for  $h=0.0, 0.1, 0.2$ , and 0.3. At  $h=0.0$  it agrees nicely with the expected behavior, whereas it is strongly affected by the finite size effects for nonzero magnetic field. This is in qualitative agreement with the theoretical finding [25] that the finite size corrections of  $P(q)$  are one order of magnitude larger in the  $q < q_m$  region than in the  $q > q_{EA}$  region, namely,

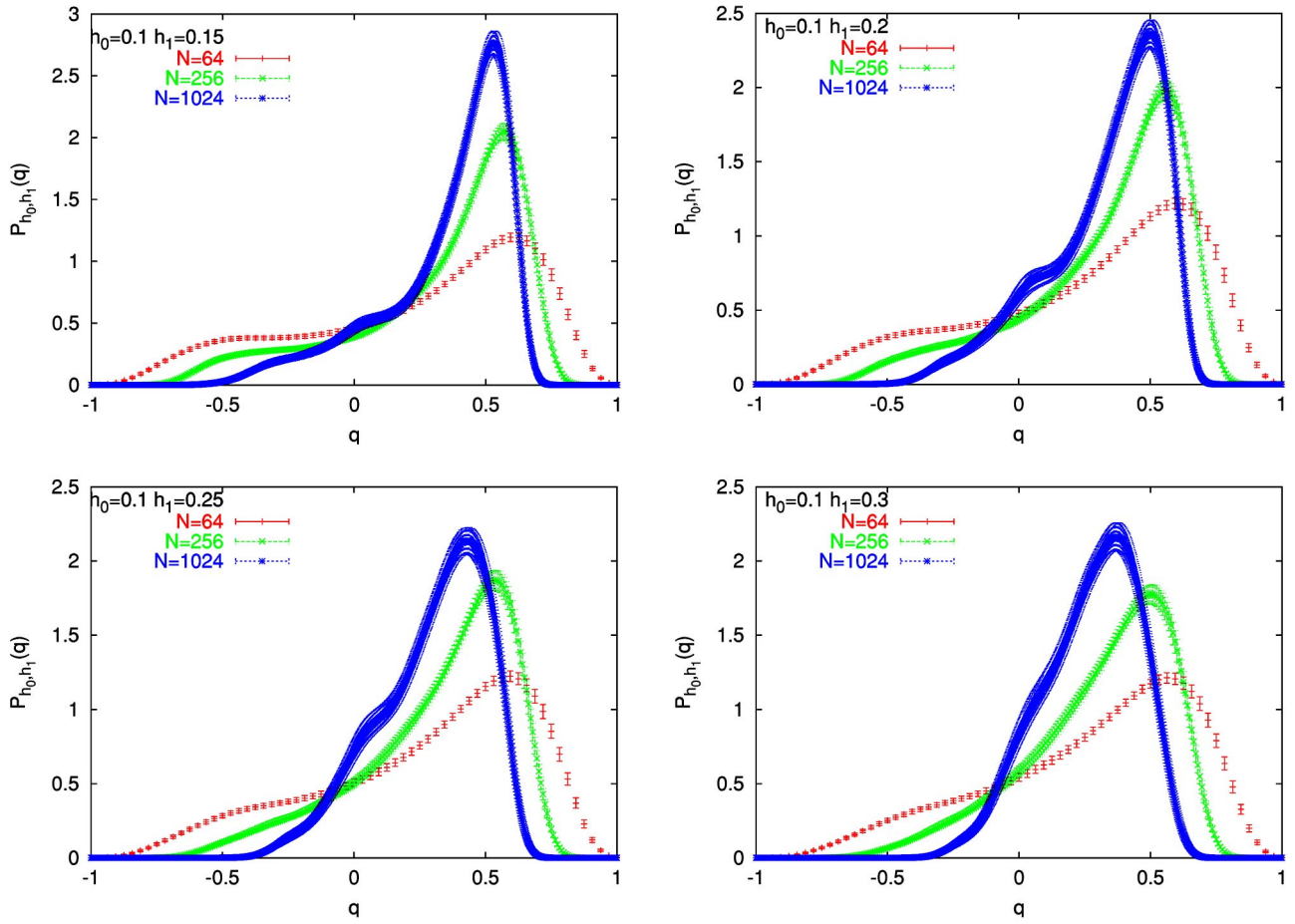


FIG. 5. The probability distribution of the overlap  $P_{h_0, h_1}(q)$  between two replicas evolving at different magnetic field values, with  $h_0 = 0.1$  and  $h_1 = 0.15, 0.2, 0.25$ , and  $0.3$ , respectively, for the considered system sizes.

$$\frac{\ln(P(q))}{N} = \begin{cases} -\lambda_m(q_m - q)^3, & q \ll q_m \\ -\lambda_{EA}(q - q_{EA})^3, & q \gg q_{EA} \end{cases} \quad (12)$$

with  $\lambda_m \ll \lambda_{EA}$ . The behavior for  $q > q_{EA}$  was tested (for  $h = 0$ ) in Refs. [26] and [27].

Here we find that for the considered sizes  $P(q)$  has a visible tail in the  $q < 0$  region for  $h$  as large as  $0.3$ . Moreover, the peak that should correspond to the thermodynamic limit  $\delta(q - q_m)$  is not visible and the expected  $\exp[-N\lambda_m(q_m - q)^3]$  behavior is swamped by the reminiscence of the  $q = -q_{EA}$  peak, still clearly visible at  $h = 0.1$ . For the increasing magnetic fields the weight of the  $q = q_m$  peak should increase (and the reminiscence of the  $q = -q_{EA}$  peak fade away) but  $q_m$  approaches  $q_{EA}$ , making difficult to distinguish between the two peaks. These kinds of strong finite size effects in a magnetic field were already observed in finite dimensional spin glasses [28,29]. Larger system sizes and/or lower temperatures would be needed in order to see the correct large volume behavior.

On the other hand, we note that in our data  $q_{EA}$  [defined as the location of the maximum of  $P(q)$ ] is practically independent of the field, as predicted by the Parisi theory (in the infinite volume limit). We obtain  $q_{EA} \approx 0.53$  for  $N = 1024$ , where a recent analytical computation [24] gives the asymptotic value  $q_{EA} \approx 0.505$  (independent of  $h$ ).

## B. On magnetic field chaos

In order to find evidences for magnetic field chaos we analyze the behavior of  $P_{h_0, h_1}(q)$ . We first consider the case  $h_0 = 0.0$  [then  $P_{0, h_1}(q)$  is still symmetric for  $q \rightarrow -q$ ] and let  $h_1$  take the values  $0.1, 0.15, 0.2$ , and  $0.3$  (see Fig. 3). Already for  $h_1 = 0.15$  we find clear evidences for a chaotic behavior when looking at the  $N = 1024$  data. This is very different from the situation one finds when looking for temperature chaos [11], where  $P_{T_0, T_1}(q \approx 0)$  does not show a clear peak corresponding to the thermodynamic limit  $\delta(q)$  for  $(T_1 - T_0)$  as large as  $0.2$  and size as large as  $N = 4096$ . It is remarkable that the appearance of the magnetic field chaos with increasing system sizes is a very sudden phenomenon: chaos is elusive for  $N = 256$  and blatant for  $N = 1024$ .

On the other hand, to get a nearly Gaussian behavior we have to consider at least  $N = 1024$  and  $h_1$  values as large as  $0.3$ , but the variance is more than an order of magnitude larger than that predicted by Eq. (8). Our data suggest that the support of  $P_{0, h}$  shrinks to 0 as  $N$  grows, and the chaotic  $q \approx 0$  peak dominates more and more the distribution.

Moreover, we find that  $A^{2n}(h_0, h_1)$  and  $B^{2n}(h_0, h_1)$ , which decrease with increasing sizes as soon as  $h_1 > 0$ , are in agreement with the expected scaling law [9], i.e.,  $\tilde{f}(Nh_1^{8/3})$ . We consider, in particular,

$$B^2(h_0, h_1, T) = \frac{\overline{\langle (q - \langle q \rangle_{h_0, h_1})^2 \rangle_{h_0, h_1}}}{\overline{\langle (q - \langle q \rangle_{h_0, h_0})^2 \rangle_{h_0, h_0}}}, \quad (13)$$

which is plotted in scaling form in Fig. 4. In the limit  $1/(Nh_1^{8/3}) \ll 1$  the scaling function approaches the asymptotic regime  $\tilde{f}(Nh_1^{8/3}) \propto 1/(Nh_1^{8/3})$  in qualitative agreement with the first-order perturbative result (8). This shows that the asymptotic regime is indeed approached in our data, and that we can safely deduce that  $\lim_{N \rightarrow \infty} B^2(0, h_1 \neq 0, T) = 0$ .

We conclude the analysis of the  $h_0 = 0$  case by looking at  $P_{h_0, h_1}(0)$  as a function of  $h_1$ . It increases when we consider increasing sizes (apart from the very small  $h$  values, where there are clearly strong finite size effects) and scales roughly as  $\tilde{f}(Nh_1^{8/3})$  (see Fig. 4) with  $\tilde{f}(Nh_1^{8/3})$  approaching the expected behavior  $\propto \sqrt{Nh_1^{8/3}}$  for  $Nh_1^{8/3} \gg 1$ . We also note that though we have plotted data only for  $h_1 \leq 0.4$ , these scaling laws appear satisfied also when we include data corresponding to  $h_1$  values on the other side of the AT line.

Next we consider  $h_0 = 0.1$ ,  $h_1 = 0.15, 0.2, 0.25$ , and  $0.3$  (see Fig. 5). The  $P_{h_0, h_1}(q)$  is still expected to approach a  $\delta$  function in the thermodynamic limit, now centered in  $q_m$  [ $q_m(h = 0.1) = 0.21$  independent of  $T$  from a recent analytical study [24]]. However, we have already noted that the peak in  $q_m$  is not evident in our data for (the usual)  $P(q)$  and correspondingly there is no clear evidence for chaotic behavior in  $P_{h_0 \neq 0, h_1}(q)$ . Also for the largest size considered, i.e.,  $N = 1024$ , though a small second peak in  $q \approx 0.05$  is appearing, the dominant contribution is still coming from the reminiscence of the peak in  $q_{EA}$ , whose mean value and height are slowly decreasing for increasing  $h_1$ . As a matter of fact, when going to the other side of the AT line, i.e.,  $h_1 \geq 0.4$ , it is this peak that survives, becoming centered on a definitely lower  $q$  value ( $\langle q \rangle_{h_0=0.1, h_1=0.6} \approx 0.18$  for  $N = 1024$ , smaller than  $q_m$ ).

It is clear that one should look at larger  $N$ 's to get evidences for the expected Gaussian shape  $\propto \exp[-(q - q_m)^2/2\sigma_{th}^2]$  (with  $1/\sigma_{th}^2 = \sqrt{2}Nh_0|h_1 - h_0|$ ) in the spin glass phase. Therefore, it is not surprising that a quantity such as  $B^2(h_0, h_1)$  does *not* scale as a function of  $N(h_1 - h_0)$ . In the case we are considering of  $h_0 = 0.1$  a form  $B^2 \sim \tilde{f}(N(h_1 - h_0)^\alpha)$  still roughly works, with  $\alpha \approx 4$ . Nevertheless, the data presented in Fig. 6 show that even for  $N = 1024$  and  $(h_1 - h_0) \approx 0.3$  we are very far from an asymptotic regime  $\tilde{f}(x) \propto 1/x$ . When looking at larger  $h_0$ ,  $B^2$  definitely does not scale, for instance, already at  $h_0 = 0.2$  we get  $B^2(N = 1024) > B^2(N = 256)$  in the whole interval  $0.2 < h_1 \leq 0.4$ .

## V. CONCLUSIONS

We performed numerical simulations of the SK model in a magnetic field at the temperature  $T = 0.6$  both in the glassy phase and above the AT line. We used a modified version of the PT algorithm in which the system is allowed to move between a chosen set of magnetic field values, an algorithm well suited for our purpose. We found that  $N = 1024$  is the

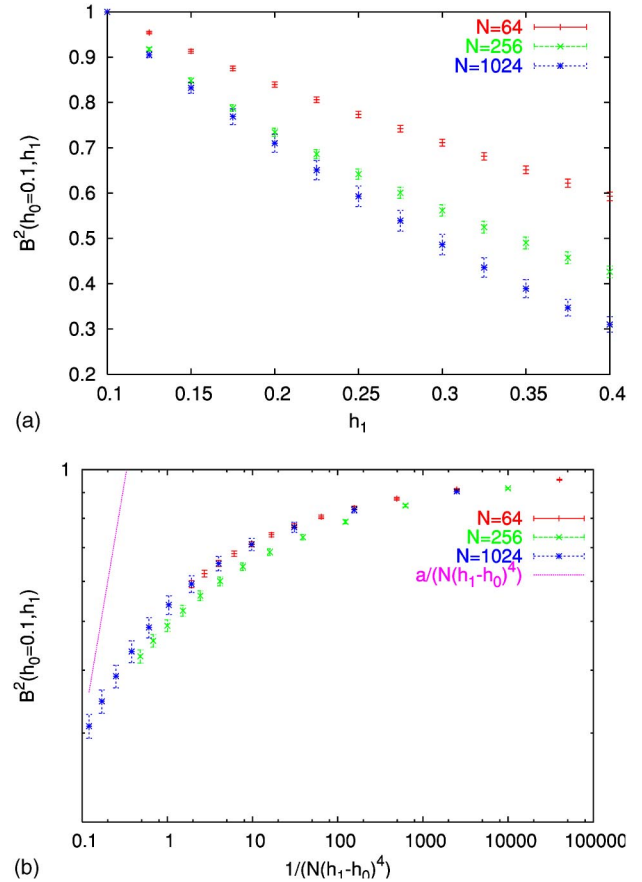


FIG. 6. The behavior of  $B^2(h_0, h_1)$  for  $h_0 = 0.1$  as a function of  $h_1$  and as a function of  $1/[N(h_1 - h_0)^4]$  compared with the asymptotic behavior  $\propto 1/[N(h_1 - h_0)^4]$  (log-log plot).

largest size one is able to efficiently thermalize with this method and we argue that this is related to the appearance of the magnetic field chaos at this scale.

The function  $P(q)$  shows strong finite size corrections for  $h > 0$ , with a long tail in the  $q < 0$  region that slowly disappears for increasing sizes, whereas the peak corresponding to the thermodynamic limit  $\delta(q - q_m)$  is not yet visible.

Our main result is on the behavior of  $P_{h_0, h_1}(q)$ , which in the case of  $h_0 = 0.0$  shows evidence for chaos already at  $h_1 = 0.15$  when we consider the still relatively small size  $N = 1024$ . This is in variance with the situation one finds when looking for temperature chaos [11], in agreement with the very recent analytical finding [17] that the temperature chaos is a much weaker effect. The appearance of the third peak in  $q = 0$  is accompanied by a shrinking of the support of the distribution.

The expected scaling law [9] is well satisfied and, for large  $Nh_1^{8/3}$ ,  $P_{h_0=0, h_1}(q)$  approaches a Gaussian with variance  $\propto 1/(Nh_1^{8/3})$ , in qualitative agreement with the result of a first-order perturbative computation [10].

On the other hand, looking at the chaotic behavior for  $h_0 \neq 0$  we found ourselves to be still very far from the expected asymptotic regime. This is to be related to the presence of strong finite size effects observable also on  $P(q)$  itself.

## ACKNOWLEDGMENTS

We acknowledge enlightening discussions with Andrea Crisanti, Cirano De Dominicis, Silvio Franz, Enzo Marinari,

Giorgio Parisi, Tommaso Rizzo, and Peter Young. B.C. is supported by Contract No. MCFI 2001-00312. We thank Andrea Crisanti and Tommaso Rizzo for providing us with their unpublished results on the  $h \neq 0$  SK model.

- 
- [1] D. Sherrington and S. Kirkpatrick, *Phys. Rev. Lett.* **35**, 1792 (1975).
- [2] G. Parisi, *Phys. Rev. Lett.* **43**, 1754 (1979); *J. Phys. A* **13**, 1101 (1980); **13**, 1887 (1980); **13**, L115 (1980).
- [3] F. Guerra and L. Toninelli, *Commun. Math. Phys.* (to be published), e-print cond-mat/0204280.
- [4] F. Guerra, e-print cond-mat/0205123.
- [5] For recent analytical results on the finite dimensional transition in magnetic field see I.R. Pimentel, T. Temesvari, and C. De Dominicis, *Phys. Rev. B* **65**, 224420 (2002); T. Temesvari and C. De Dominicis, *Phys. Rev. Lett.* **89**, 97204 (2002).
- [6] For a review see E. Marinari, G. Parisi, F. Ricci-Tersenghi, J. Ruiz-Lorenzo, and F. Zuliani, *J. Stat. Phys.* **98**, 973 (2000).
- [7] I. Kondor, *J. Phys. A* **22**, L163 (1989).
- [8] I. Kondor and A. Végő, *J. Phys. A* **26**, L641 (1993).
- [9] F. Ritort, *Phys. Rev. B* **50**, 6844 (1994).
- [10] M. Ney-Nifle, *Phys. Rev. B* **57**, 492 (1998).
- [11] A. Billoire and E. Marinari, *J. Phys. A* **33**, L265 (2000); *Europhys. Lett.* **60**, 775 (2002).
- [12] T. Rizzo, *J. Phys. A* **34**, 5531 (2001).
- [13] R. Mulet, A. Pagnani, and G. Parisi, *Phys. Rev. B* **63**, 184438 (2001).
- [14] F. Krzakala and O.C. Martin, *Eur. Phys. J. B* **28**, 199 (2002).
- [15] M. Sales and H. Yoshino, *Phys. Rev. E* **65**, 66131 (2002).
- [16] M. Sasaki and O.C. Martin, e-print cond-mat/0206316.
- [17] A. Crisanti and T. Rizzo, e-print cond-mat/0209333.
- [18] G. Parisi, *Phys. Rev. Lett.* **50**, 1946 (1983); *Physica A* **124**, 523 (1984).
- [19] J.R.L. de Almeida and D.J. Thouless, *J. Phys. A* **11**, 983 (1978).
- [20] M.C. Tesi, E. Janse van Rensburg, E. Orlandini, and S.G. Whittington, *J. Stat. Phys.* **82**, 155 (1996); K. Hukushima and K. Nemoto, *J. Phys. Soc. Jpn.* **65**, 1604 (1996).
- [21] See, for instance, E. Marinari, in *Advances in Computer Simulations*, edited by J. Kerstéz and I. Kondor (Springer, Berlin, 1998); e-print cond-mat/9612010.
- [22] M. Mézard, G. Parisi, and M.A. Virasoro, *Spin Glass Theory and Beyond* (World Scientific, Singapore, 1987).
- [23] K. Binder and A.P. Young, *Rev. Mod. Phys.* **58**, 801 (1986).
- [24] A. Crisanti and T. Rizzo, e-print cond-mat/0111037.
- [25] S. Franz, G. Parisi, and M.A. Virasoro, *J. Phys. I* **2**, 1869 (1992).
- [26] G. Parisi, F. Ritort, and F. Slanina, *J. Phys. A* **26**, 3775 (1993).
- [27] A. Billoire, S. Franz, and E. Marinari, *J. Phys. A* **36**, 15 (2002).
- [28] J.C. Ciria, G. Parisi, F. Ritort, and J.J. Ruiz-Lorenzo, *J. Phys. I* **3**, 2207 (1993).
- [29] M. Picco and F. Ritort, *J. Phys. I* 1619 (1994).